ISSN 2411-3336; e-ISSN 2541-9404

JOURNAL OF MINING INSTITUTE

Zapiski Gornogo instituta

Journal homepage: pmi.spmi.ru

Research article *Geology*

Mineralogical and geochemical characteristics of coals from the Mugun deposit and sediment provenance during their formation

Danzan B. Bembeev[1]✉, **Sofya I. Merenkova**[2,3], **Aleksei A. Samsonov**[1], **Ruslan R. Gabdullin**[1,4]

[1] *Lomonosov Moscow State University, Moscow, Russia*

[2] *Shirshov Institute of Oceanology of RAS, Moscow, Russia*

[3] *Schmidt Institute of Physics of the Earth of the RAS, Moscow, Russia*

[4] *Vernadsky Institute of Geochemistry and Analytical Chemistry of the RAS, Moscow, Russia*

How to cite this article: Bembeev D.B., Merenkova S.I., Samsonov A.A., Gabdullin R.R. Mineralogical and geochemical characteristics of coals from the Mugun deposit and sediment provenance during their formation. Journal of Mining Institute. 2026. Vol. 280, p. 85-103.

Abstract

This study presents a comprehensive mineralogical and geochemical investigation of lignites from the Mugun deposit within the Irkutsk Coal Basin. The relevance of the research is determined by the need for the rational utilization of coal resources amid growing interest in the recovery of valuable and potentially valuable trace elements, including Ge, Ga, Sc, REE, U, and others, from coal and coal combustion products. The study aims to identify the distribution patterns of trace elements in coals and host rocks, determine their modes of occurrence, and reconstruct the provenance of the sedimentary material that formed the coal-bearing sequence. The research employed a combination of analytical methods, including X-ray fluorescence analysis, mass spectrometry, and scanning electron microscopy, together with statistical approaches such as correlation analysis and principal component analysis. It was established that trace-element enrichment in the coals resulted from clastic, biogenic, diagenetic, and epigenetic processes. The principal trace-element-bearing phases include clay minerals, particularly kaolinite, as well as sulfides, phosphates, and organic matter. Discriminant analysis of the composition of terrigenous rock interlayers, represented by siltstones and mudstones occurring between the coal seams, made it possible to reconstruct the sediment sources. These included granitoids and felsic and subalkaline volcanic rocks exposed in the foothills of the Eastern Sayan. The results provide a basis for proposing a highly plausible model of the coal-forming conditions and for predicting the distribution of trace elements in the coals and host rocks.

Keywords

Mugun deposit; lignite; geochemistry; trace elements; ash yield; mineralogy; principal component analysis; sediment provenance

Funding

The study was conducted within the framework of the State assignment of Lomonosov Moscow State University and was partially funded under the State assignment of Shirshov Institute of Oceanology of RAS (FMWE-2024-0020), as well as the State assignments of Vernadsky Institute of Geochemistry and Analytical Chemistry of the RAS, and Schmidt Institute of Physics of the Earth of the RAS.

Received: 06.10.2025 ***Accepted: 28.04.2026*** ***Online: 24.07.2026*** ***Published: 10.09.2026***

Introduction

The relevance of studying the geochemistry of lignite is determined by several factors. In recent years, the integrated processing of coal resources has become increasingly important. This approach involves not only utilizing the energy potential of coal itself, but also recovering critical elements, such as Ge, Ga, REE, and others, from coal and coal combustion wastes. Anomalous concentrations of several valuable rare and non-ferrous metals, including Ti, Zr, V, W, Y, Co, Ga, Ge, Nb, and Be, have been reported in deposits of the Kuznetsk Basin. These concentrations are most commonly associated with zones of tectonic disruption within coal seams, particularly where the seams occur near intrusive bodies [1, 2]. The successful recovery of REE from coal ash may improve the economic efficiency of the thermal power industry by creating additional sources of revenue [3, 4]. The environmental implications are also of particular importance. Large-scale coal mining and combustion result in the accumulation of ash and slag wastes, which, in the absence of proper disposal or utilization, may become a source of particulate emissions into the biosphere. Accordingly, studies of the mineralogical and elemental composition of coals, ashes, and slags are essential for developing approaches to reducing anthropogenic impacts and improving the efficiency of coal-resource utilization. In addition to their practical importance, investigations into the accumulation patterns of trace elements in coal are of fundamental scientific interest because they contribute to the reconstruction of coal accumulation and coal-forming conditions in the region under consideration [5].

The Mugun lignite deposit forms part of the Irkutsk Coal Basin, a major coal-bearing region that has served as one of the sources of fuel and energy resources for Eastern Siberia for many decades. Over recent decades, understanding of the geochemical and mineralogical characteristics of coals from the Mugun deposit has expanded considerably. Previous studies [6-8] have shown that, in addition to their energy potential, the local lignites contain rare mineral inclusions and coal-affinitive elements, whereas the ash and slag wastes produced during combustion are enriched in certain strategically important metals. However, the principal concentrators and modes of occurrence of valuable elements remain insufficiently characterized, and a comprehensive assessment of their recovery efficiency is still lacking. Addressing these issues may contribute to improving the economic viability of the Mugun deposit and to more complete utilization of the region's resource potential.

Brief geological setting and study materials

The Mugun lignite deposit is located in the Tulun District of Irkutsk Region, 40 km southwest of the town of Tulun, on the gently sloping watershed between the Kurzanka and Manut rivers, tributaries of the larger Iya River (Fig.1). The deposit lies within the southern part of the Siberian Platform and is characterized by a relatively simple geological structure. Lower Paleozoic deposits occur here in nearly horizontal or gently undulating attitudes and are intruded by lens-shaped sill-like bodies. Nearly horizontal, unconsolidated Jurassic freshwater sedimentary rocks overlie the eroded surface of this basement. Post-Jurassic erosion deeply dissected the sedimentary succession, particularly the Jurassic deposits. The latter have been preserved either on watersheds or within depressions in the surface of the Paleozoic basement, which have highly irregular outlines. Depending on the depth of erosion, different stratigraphic units are exposed at the present-day surface [9].

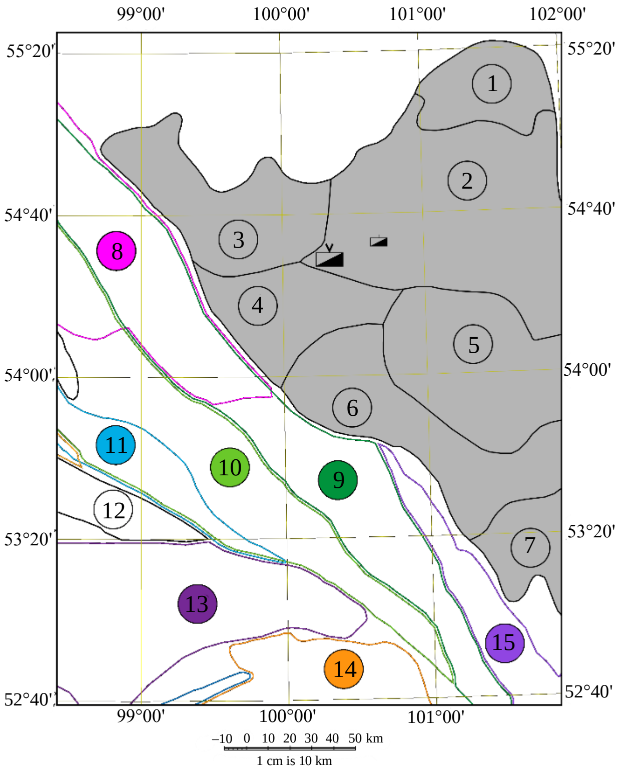

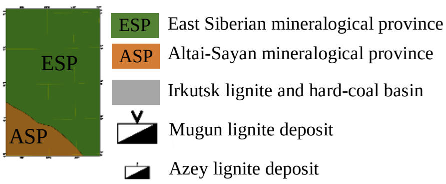

Fig.1. Location of the Mugun deposit relative to the East Siberian and Altai-Sayan mineralogical provinces. Compiled from a fragment of the State Geological Map of the Russian Federation, Sheet N-47 [10]

1-7 – districts of the Irkutsk lignite and hard-coal basin: 1 – Khakhareisky coal district, 2 – Tulunsky lignite district, 3 – Budagovo-Udinsky coal district, 4 – Ikeysky hard-coal district, 5 – Karantsaisky hard-coal district, 6 – Verkhneziminsky prospective hard-coal district, 7 – Central Prisayanskii hard-coal district; 8-15 – metallogenic zones: 8 – Prisayanskaya uranium-phosphorite-manganese ore zone, 9 – Urik-Tumanshet uranium-gold-rare-metal ore zone, 10 – Biryusinskaya muscovite-rare-earth-nickel ore zone, 11 – Ognitskaya gold-uranium-molybdenum-lead ore zone, 12 – Derbinskaya manganese-graphite zone, 13 – Utkhum-Khamsara gold-lead-iron ore zone, 14 – Urik-Kitoy-Bokson phosphorite-vanadium-gold ore zone, 15 – Sharyzhalgai alumina-iron ore zone

Structurally, the area may be divided into two zones: the platform zone proper and the foreland-depression zone. The platform zone occupies the northeastern part of the area. It is characterized by a relatively limited thickness of coal-bearing Jurassic deposits, which were preserved from erosion within depressions in the comparatively stable Paleozoic basement. The Jurassic succession reaches a thickness of up to 150 m in this zone. The southern boundary of the platform zone may conventionally be traced along the southern boundary of the Mugun deposit [11]. To the southwest, the platform zone gradually passes into the foreland-depression zone, which is bordered to the south by the folded region of the Eastern Sayan. The immediate proximity of the folded belt promoted mobility of the pre-Jurassic basement during deposition of the Jurassic succession. As a result, the thickness of the coal-bearing deposits increases in the central part of the zone and reaches 200-300 m in some parts of the foreland depression. The geological succession of the area and the deposit comprises Paleozoic and Mesozoic sedimentary units overlain by Quaternary deposits [11]:

• the Paleozoic complex, composed mainly of Ordovician sandstones, siltstones, mudstones, and trap intrusions, forms an irregularly dissected pre-Jurassic basement;

• the Mesozoic complex is represented by Middle Jurassic deposits of the Zalarinskaya, Cheremkhovskaya, and Prisajanskaya formations, with coal-bearing seams occurring in erosional-tectonic depressions; the productive, or Cheremkhovskaya, Formation contains several principal mineable lignite seams;

• Quaternary deposits, represented by alluvial and eluvial-deluvial sediments, continuously cover the sedimentary sequence; they are relatively thin on watersheds and become thicker in valleys.

The Jurassic deposits of the Mugun deposit occur within an erosional-tectonic depression in the Paleozoic basement and comprise three formations: the Zalarinskaya (J_1*zl*), Cheremkhovskaya ($J_{1\text{-}2}$*cr*), and Prisajanskaya (J_2*ps*). The barren Zalarinskaya Formation, 0-53 m thick, consists of quartz sandstones, siltstones, and less commonly conglomerates, and contains no commercially significant coal seams. The Prisajanskaya Formation, 0-20 m thick, likewise contains no mineable coal seams, although it may include isolated thin coal lenses.

According to P.P.Timofeev [12], the Cheremkhovskaya coal-bearing formation accumulated in a continental freshwater basin dominated by swampy plains alternating with lacustrine-alluvial systems. These conditions favored the formation of thick coal seams interbedded with terrigenous deposits represented mainly by siltstones and mudstones. In some cases, transitional varieties of terrigenous rocks compositionally similar to clay-rich rocks occur. Hereafter, these are conventionally referred to as terrigenous interlayers.

The Cheremkhovskaya Formation, 60-85 m thick, is of primary importance for the commercial coal potential of the deposit and is divided into three horizons:

• the lower, non-commercial horizon, composed of polymictic sandstones with rare thin coal lenses;

• the productive-seam horizon, comprising sandstones, siltstones, mudstones, and coal seams of mineable thickness;

• the upper, non-commercial horizon, dominated by sandstones with occasional lenses of carbonaceous rocks.

Thus, all commercially significant coal reserves of the Mugun deposit are confined to the productive-seam horizon of the Cheremkhovskaya Formation, specifically Seams I and II. Coal sampling was carried out within the Mugun deposit, where the Southern, Western, and Central blocks, as well as the boundary trench of the Central Block, were being mined at the time of the study. Seams I, II, and IIa were under development. Sampling locations were selected with due consideration of the current mining and technical conditions. During sampling, a considerable part of the section was inaccessible because drainage ditches were flooded and some areas were characterized by an increased risk of rock collapse. Navigation was performed using built-in smartphone GPS modules and the SpotLens and GPS Camera applications; coordinates were recorded in the UTM WGS84 coordinate system.

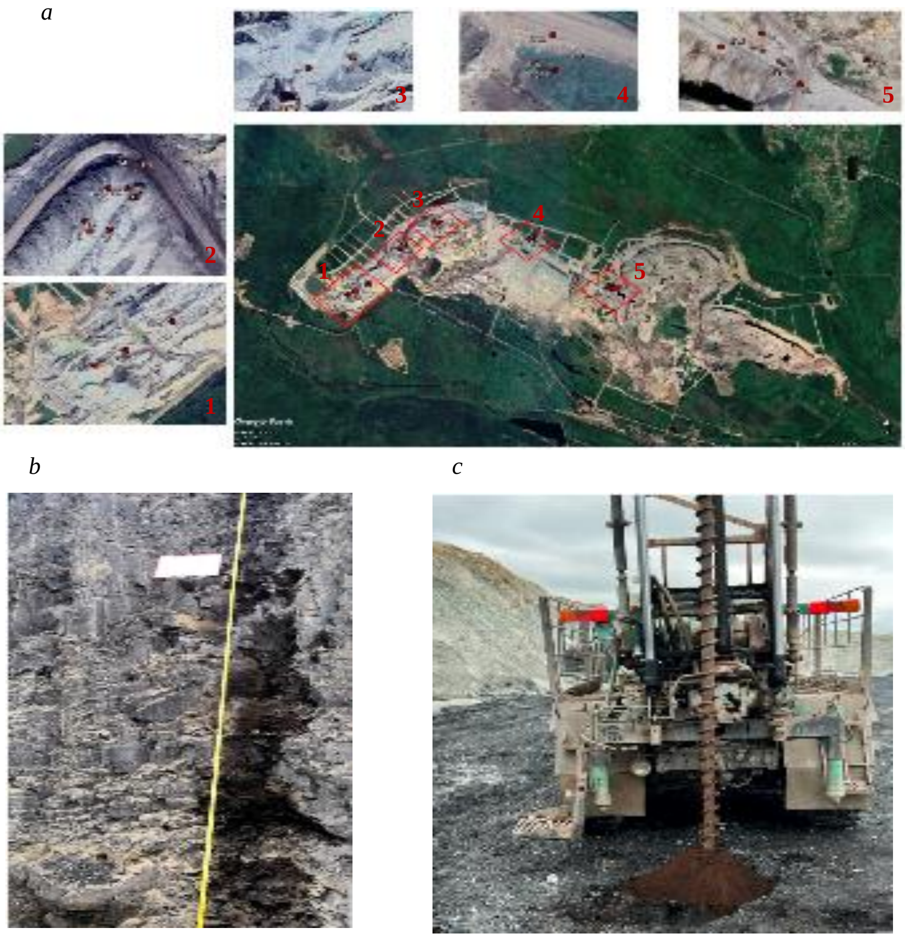

Fig.2. Map showing the locations of the sampling sites (*a*) and sampling methods at the Mugun deposit: *b* – manual; *c* – drilling

Sampling was conducted at five sites, numbered 1-5 (Fig.2, *a*), located within the Southern, Western, and Central blocks of the Mugun deposit. Sites 1 and 2 were situated within the Southern Block: Site 1 was located in its southern part and included three sampling points, whereas Site 2 was located in its northern part and included eight sampling points. Sites 3-5 were located within the Western and Central blocks: Site 3 was situated in the western part of the Western Block near the boundary with the Southern Block and included three sampling points, Site 4 was located in the central part of the Western Block and included four points, and Site 5 was situated in the western part of the Central Block near the boundary with the Western Block and included six points.

Samples were collected along the active mining front with due regard for the prevailing mining and technical conditions. Each sampling record included information on seam thickness, the characteristics of individual benches, the lithological composition of the sampled material, and the sample type, either differential or production. Differential samples were collected for subsequent investigation of element distribution within individual benches. In some cases, samples were also taken from the seam roof, floor, and thick interbeds for comparison with the main coal body.

Sampling was performed both manually and by drilling. Manual sampling employed the channel-sampling method, in which the geometric dimensions of the channel, approximately 10 cm in both width and depth, were used as a guide to ensure uniform coverage of the sampled interval (Fig.2, *b*). The material was collected on a tarpaulin placed beneath the sampling point and then packed into bags containing identification sheets. The samples were subsequently transported to the technical quality-control department, where they were crushed to a particle size of less than 3 mm, reduced, and packed into airtight zip-lock bags. Auger drilling was used for drill sampling; the samples were also reduced on site and packed into similar bags (Fig.2, *c*). After crushing and reduction, the average mass of a laboratory sample was approximately 600 g.

Photographic documentation of the actual sampling location was prepared at each sampling point (Fig.2, *b*, *c*). Figure 2, *b* shows a transverse channel approximately 3.7 m long, 10 cm wide, and 10 cm deep, from which a manual sample was collected by channel sampling. Figure 2, *c* illustrates drill sampling: an auger drill was advanced into the coal seam to a depth of up to 4.5 m, after which the recovered core material was used to prepare a sample of comparable mass.

A total of 89 samples were collected from 24 sampling points within the Mugun deposit (Fig.2, *a*). In the Southern Block, 41 samples were collected from 11 points, including nine manually collected samples from Seam I at two points, five manually collected samples from Seam II at one point, and 27 drill samples from eight points.

In the Western Block, 29 samples were collected from seven points, including 25 drill samples from Seam I at six points and four manually collected samples from Seam II at one point.

In the Central Block, 19 samples were collected from six points, including nine manually collected samples from Seam I at three points and 10 drill samples from three points. No sampling was conducted within the boundary trench of the Central Block because no accessible exposed sections were available. Sampling-point and sample numbers are listed in Table 1.

Table 1

Sampling locations and sample numbers from the Mugun deposit

Sampling location	Sample	Sampling location	Sample	Sampling location	Sample	Sampling location	Sample
Mu1	Mu-D-1-1-1	B3	Mu-D-B3-2-1	M3	M-D-3-1-1	B12	M-D-B12-1-1
	Mu-D-1-1-2		Mu-D-B3-2-2		M-D-3-1-2		M-D-B12-1-2
	Mu-D-1-1-3		Mu-D-B3-2-3		M-D-3-1-3		M-D-B12-1-3
	Mu-D-1-1-4	B4	Mu-D-B4-2-1	M4	M-D-4-1-1		M-D-B12-1-4
	Mu-D-1-1-5		Mu-D-B4-2-2		M-D-4-1-2	B13	M-D-B13-1-1
Mu2	Mu-D-2-1-1		Mu-D-B4-2-3		M-D-4-1-3		M-D-B13-1-2
	Mu-D-2-1-2	B5	Mu-D-B5-2-1	M5	M-D-5-2-1		M-D-B13-1-3
	Mu-D-2-1-3		Mu-D-B5-2-2		M-D-5-2-2		M-D-B13-1-4
	Mu-D-2-1-4		Mu-D-B5-2-3		M-D-5-2-3	B14	M-D-B14-1-1
Mu3	Mu-D-3-2-1	B6	Mu-D-B6-2-1		M-D-5-2-4		M-D-B14-1-2
	Mu-D-3-2-2		Mu-D-B6-2-2	B9	M-D-B9-1-1		M-D-B14-1-3
	Mu-D-3-2-3		Mu-D-B6-2-3		M-D-B9-1-2		M-D-B14-1-4
	Mu-D-3-2-4	B7	Mu-D-B7-2-1		M-D-B9-1-3	B15	M-D-B15-1-1
	Mu-D-3-2-5		Mu-D-B7-2-2		M-D-B9-1-4		M-D-B15-1-2
B1	Mu-D-B1-2-1		Mu-D-B7-2-3		M-D-B9-1-5		M-D-B15-1-3
	Mu-D-B1-2-2		Mu-D-B7-2-4	B10	M-D-B10-1-1	B16	M-D-B16-1-1
	Mu-D-B1-2-3	B8	Mu-D-B8-2-1		M-D-B10-1-2		M-D-B16-1-2
	Mu-D-B1-2-4		Mu-D-B8-2-2		M-D-B10-1-3		M-D-B16-1-3
B2	Mu-D-B2-2-1		Mu-D-B8-2-3		M-D-B10-1-4		M-D-B16-1-4
	Mu-D-B2-2-2		Mu-D-B8-2-4	B11	M-D-B11-1-1	B17	M-D-B17-1-1
	Mu-D-B2-2-3	M2	M-D-2-1-1		M-D-B11-1-2		M-D-B17-1-2
			M-D-2-1-2		M-D-B11-1-3		M-D-B17-1-3
			M-D-2-1-3		M-D-B11-1-4		

Research methods

X-ray fluorescence (XRF) analysis was performed using a PANalytical Axios mAX wavelength-dispersive spectrometer operated under vacuum. The method is based on excitation of atoms in the analyzed sample by X-rays and measurement of the characteristic fluorescent radiation emitted by the constituent elements. The spectrometer was equipped with a 4 kW X-ray tube with an Rh anode, with a maximum accelerating voltage of 60 kV and a maximum anode current of 160 mA. The analyses were carried out using procedures approved by the Federal Scientific and Methodological Centre for Laboratory Research and Certification of Mineral Raw Materials "VIMS". The results correspond to accuracy category III for quantitative analysis in accordance with OST RF 41-08-205-04.

Inductively coupled plasma mass spectrometry (ICP-MS) following acid digestion was performed using an Agilent MS7900 quadrupole mass spectrometer. The samples were digested in a mixture of nitric and hydrochloric acids (aqua regia), after which the elements in the resulting solutions were determined by high-sensitivity ICP-MS analysis.

Photomicrographs and X-ray spectral microanalysis were obtained at the Shared Research Facilities Centre of Schmidt Institute of Physics of the Earth of the RAS, using a TESCAN MIRA LMS scanning electron microscope (SEM) equipped with an Ultim Max 65 energy-dispersive X-ray (EDX) spectrometer and integrated AZtecLive Automated software (Oxford Instruments). The analyses were conducted at an accelerating voltage of 20 KeV and a working distance of 15 mm.

Principal component analysis (PCA) was applied to the trace-element concentration data to identify correlations among the elements. PCA is a widely used statistical technique that transforms interrelated variables into a set of independent, orthogonal components. When applied to geochemical data, PCA simplifies the analysis of multidimensional datasets, reveals latent patterns in element distribution, and assists in interpreting the factors controlling their accumulation.

The ash yield of the coal samples was determined by the slow-ashing reference method in accordance with GOST R 55661-2013. The method involves combustion of a weighed fuel sample under free access of air, followed by ignition of the ash residue to constant mass at 815±10 °C. The analysis was performed on air-dried samples. The ash yield of each analytical sample was calculated using the standard formula and expressed as a percentage; the reported value was taken as the arithmetic mean of two parallel determinations.

Results

The XRF and ICP-MS data were summarized using the principal descriptive statistical parameters, which made it possible to characterize variations in element concentrations and identify their distribution patterns within the Mugun deposit. The summary statistics are presented in Tables 2-4. Table 2 includes 89 samples, Table 3 includes 74 samples, and Table 4 includes 15 samples. Trace-element concentrations in the coals were determined from the chemical-analysis results. To assess the degree of element enrichment, the measured concentrations were compared with world coal Clarke values (C) [13], which represent average element concentrations in coals. Sulfur is an exception because its coal Clarke value cannot be determined empirically.

Table 2

Statistical characteristics of trace-element concentrations in coal and host-rock samples

Element	Min	Max	Mean	Median	σ*	CV**
Ash yield, %	3.8	86.9	22.4	13.9	20.0	89.0
Li, ppm	2.4	153.4	37.4	24.4	33.1	89.0
Be, ppm	0.6	3.9	1.7	1.4	0.8	48.0
B, ppm	40.4	243.6	147.2	148.7	40.4	27.0
Sc, ppm	0.9	47.4	8.4	4.5	9.5	113.0

End of Table 2

Element	Min	Max	Mean	Median	σ*	CV**
Ti, %	0.005	0.6	0.1	0.1	0.1	126.0
V, ppm	14.5	315.9	70.0	54.2	51.5	74.0
Cr, ppm	3.6	118.3	32.5	21.8	27.8	85.0
Mn, ppm	29.3	366.3	107.9	89.4	64.1	59.0
Fe, %	0.2	4.0	0.9	0.6	0.7	79.0
Ni, ppm	6.5	81.2	18.1	13.5	12.6	69.0
Cu, ppm	8.8	499.5	50.1	30.4	70.7	141.0
Zn, ppm	1.2	158.6	37.7	21.2	39.2	104.0
Ga, ppm	1.0	24.4	7.7	5.3	6.0	78.0
Ge, ppm	0.3	35.2	3.1	1.0	6.2	199.0
As, ppm	0.2	87.1	5.3	2.8	10.3	193.0
Rb, ppm	0.1	99.4	13.6	2.5	23.3	171.0
Sr, ppm	3.6	283.7	87.4	91.4	48.4	55.0
Y, ppm	1.3	50.1	18.2	16.7	10.0	55.0
Zr, ppm	3.9	192.8	52.3	36.7	43.1	83.0
Nb, ppm	0.1	19.9	4.4	2.9	4.4	99.0
Mo, ppm	0.4	5.2	1.3	1.0	0.9	68.0
Ag, ppm	0.015	0.297	0.075	0.047	0.08	101.0
Cd, ppm	0.015	1.644	0.295	0.221	0.28	94.0
Sn, ppm	0.015	3.839	1.241	0.969	0.97	78.0
Sb, ppm	0.015	1.697	0.332	0.288	0.25	75.0
Cs, ppm	0.015	6.238	0.899	0.199	1.49	165.0
Ba, ppm	18.7	648.0	82.8	45.6	110.6	134.0
Hf, ppm	0.039	5.703	1.595	1.248	1.20	75.0
Ta, ppm	0.015	1.460	0.351	0.248	0.33	93.0
Pb, ppm	0.5	24.6	7.2	5.9	5.2	72.0
Th, ppm	0.4	16.4	4.8	3.4	3.9	80.0
U, ppm	0.2	7.9	2.3	2.0	1.4	62.0
W, ppm	2.8	169.9	19.5	11.7	24.4	125.0
P, %	0.001	0.093	0.01	0.005	0.01	133.0
S, %	0.2	5.4	1.7	0.9	1.4	83.0
Cl, %	0.004	0.009	0.005	0.005	0.002	30.0
F, %	0.005	0.064	0.016	0.01	0.02	96.0

* σ – standard deviation.
** CV – coefficient of variation, %.

Table 3

Statistical characteristics of trace-element concentrations in coal samples

Element	Min	Max	Mean	Median	σ	CV
Ash yield, %	3.8	37.8	14.1	12.2	6.6	47.0
Li, ppm	2.4	72.7	25.3	21.5	14.2	56.2
Be, ppm	0.6	3.9	1.5	1.3	0.6	44.2
B, ppm	93.1	243.6	158.9	155.4	30.7	19.3
Sc, ppm	0.9	36.9	5.7	3.7	6.6	115.4
Ti, %	0.005	0.199	0.057	0.035	0.048	84.5

End of Table 3

Element	Min	Max	Mean	Median	σ	CV
V, ppm	14.5	216.2	58.0	49.0	41.0	71.0
Cr, ppm	3.6	64.2	21.8	18.4	14.0	64.3
Mn, ppm	29.3	366.3	99.9	87.5	63.6	63.6
Fe, %	0.2	4.0	0.7	0.6	0.5	67.9
Ni, ppm	6.5	81.2	14.7	12.2	9.9	67.5
Cu, ppm	8.8	499.5	48.6	26.3	75.4	155.1
Zn, ppm	1.2	158.6	28.8	18.5	33.3	115.6
Ga, ppm	1.0	14.7	5.5	4.7	3.0	55.5
Ge, ppm	0.3	33.1	2.2	0.8	4.8	223.1
As, ppm	0.2	87.1	4.4	2.1	10.8	245.3
Rb, ppm	0.1	32.2	4.5	2.1	6.0	134.4
Sr, ppm	3.6	283.7	90.9	94.1	49.6	54.6
Y, ppm	1.3	50.1	16.2	14.0	9.0	55.4
Zr, ppm	3.9	90.2	36.7	33.3	19.6	53.4
Nb, ppm	0.1	7.8	2.8	2.5	1.6	57.2
Mo, ppm	0.6	4.3	1.2	1.0	0.7	57.9
Ag, ppm	0.015	0.162	0.047	0.015	0.042	89.6
Cd, ppm	0.015	1.644	0.282	0.201	0.295	104.8
Sn, ppm	0.015	3.839	0.974	0.772	0.762	78.2
Sb, ppm	0.015	1.270	0.286	0.227	0.194	67.8
Cs, ppm	0.015	3.549	0.349	0.129	0.580	166.3
Ba, ppm	18.7	109.3	43.3	42.9	16.9	38.9
Hf, ppm	0.039	2.806	1.180	1.091	0.607	51.4
Ta, ppm	0.015	0.731	0.241	0.206	0.162	67.4
Pb, ppm	0.5	14.2	5.6	5.2	3.1	55.8
Th, ppm	0.4	14.1	3.7	2.9	2.9	77.5
U, ppm	0.2	7.9	2.0	1.8	1.3	64.9
W, ppm	2.8	69.6	14.6	11.1	13.3	91.3
P, %	0.001	0.046	0.007	0.005	0.008	117.3
S, %	0.6	5.4	1.7	0.9	1.4	82.6
Cl, %	0.004	0.008	0.005	0.005	0.001	17.1
F, %	0.005	0.033	0.010	0.005	0.008	74.0

Table 4

Statistical characteristics of trace-element concentrations in host-rock samples

Element	Min	Max	Mean	Median	σ	CV
Ash yield, %	39.5	86.9	63.1	61.3	12.2	19.3
Li, ppm	25.9	153.4	97.3	102.6	35.1	36.1
Be, ppm	0.9	3.9	2.6	2.7	0.8	31.1
B, ppm	40.4	148.7	89.4	88.1	32.4	36.2
Sc, ppm	11.0	47.4	21.5	19.7	10.7	49.4
Ti, %	0.194	0.587	0.395	0.379	0.125	31.7
V, ppm	73.6	315.9	129.5	113.7	57.2	44.2
Cr, ppm	65.4	118.3	84.9	84.5	16.5	19.4
Mn, ppm	55.0	239.0	147.3	138.5	52.5	35.7
Fe, %	0.6	3.9	1.9	1.9	0.8	42.3

End of Table 4

Element	Min	Max	Mean	Median	σ	CV
Ni, ppm	14.9	54.5	35.2	35.9	10.3	29.1
Cu, ppm	9.3	188.4	57.5	48.9	41.3	71.8
Zn, ppm	18.9	141.2	81.8	86.5	37.5	45.8
Ga, ppm	8.9	24.4	18.6	19.9	4.8	26.0
Ge, ppm	1.3	35.2	7.8	3.6	9.6	122.8
As, ppm	1.4	21.2	10.0	9.8	5.6	55.6
Rb, ppm	11.2	99.4	58.8	58.7	24.6	41.8
Sr, ppm	16.7	136.0	70.3	76.6	38.3	54.4
Y, ppm	14.0	45.8	28.2	28.8	8.9	31.6
Zr, ppm	57.5	192.8	129.3	140.6	45.4	35.1
Nb, ppm	2.8	19.9	12.4	12.3	5.0	40.7
Mo, ppm	0.4	5.2	2.0	1.6	1.4	71.1
Ag, ppm	0.115	0.297	0.211	0.214	0.048	22.5
Cd, ppm	0.104	0.794	0.363	0.306	0.164	45.3
Sn, ppm	0.833	3.610	2.561	2.758	0.829	32.4
Sb, ppm	0.180	1.697	0.558	0.510	0.352	63.2
Cs, ppm	0.574	6.238	3.613	3.846	1.618	44.8
Ba, ppm	72.6	648.0	277.8	239.5	162.6	58.5
Hf, ppm	1.452	5.703	3.643	4.015	1.290	35.4
Ta, ppm	0.204	1.460	0.896	0.917	0.383	42.7
Pb, ppm	5.3	24.6	15.2	15.2	5.8	38.5
Th, ppm	4.5	16.4	10.3	9.3	3.6	34.9
U, ppm	1.1	4.8	3.7	4.1	1.1	29.3
W, ppm	4.6	169.9	43.8	26.2	45.3	103.5
P, %	0.012	0.093	0.029	0.021	0.021	73.5
S, %	0.2	4.0	1.6	0.7	1.4	86.0
Cl, %	0.007	0.009	0.008	0.008	0.001	7.4
F, %	0.012	0.064	0.043	0.045	0.014	32.7

Based on comparison of the analytical data with the Clarke values, concentration coefficients (Cc) were calculated to characterize the degree of enrichment or depletion of the coals relative to the global background. The mean Cc was defined as the ratio of the arithmetic mean concentration of an element in the entire sample set to its world coal Clarke value and was used to assess the overall level of element accumulation in the coals of the deposit.

A geochemical spectrum of coals from the Mugun deposit was constructed from the calculated concentration coefficients (Fig.3). For interpretation, the elements were grouped according to their Cc values. The geochemical spectrum showed that the mean concentrations of Li, B, V, Cr, Cu, and Er exceeded the corresponding world coal Clarke values by factors of 2.5-3.2, whereas W exceeded its Clarke value by a factor of 12.2. These elements may therefore be regarded as potentially significant targets for further investigation of their modes of occurrence and distribution.

Mineralogical characteristics. SEM observations identified the following mineral inclusions in coals from the Mugun deposit. The most common phases are kaolinite (Fig.4, *a*), which probably formed through alteration of feldspars, as indicated by shapes inherited from the original grains, as well as pyrite and quartz (Fig.4, *b*). In addition to quartz, the allogenic components include zircon containing Hf and rutile (Fig.4, *c*, *f*). Fractures contain magnetite with Zn and Al impurities (Fig.4, *d*), oxidized galena (possibly anglesite) with chalcopyrite inclusions (Fig.4, *e*), calcite (Fig.4, *g*), apatite

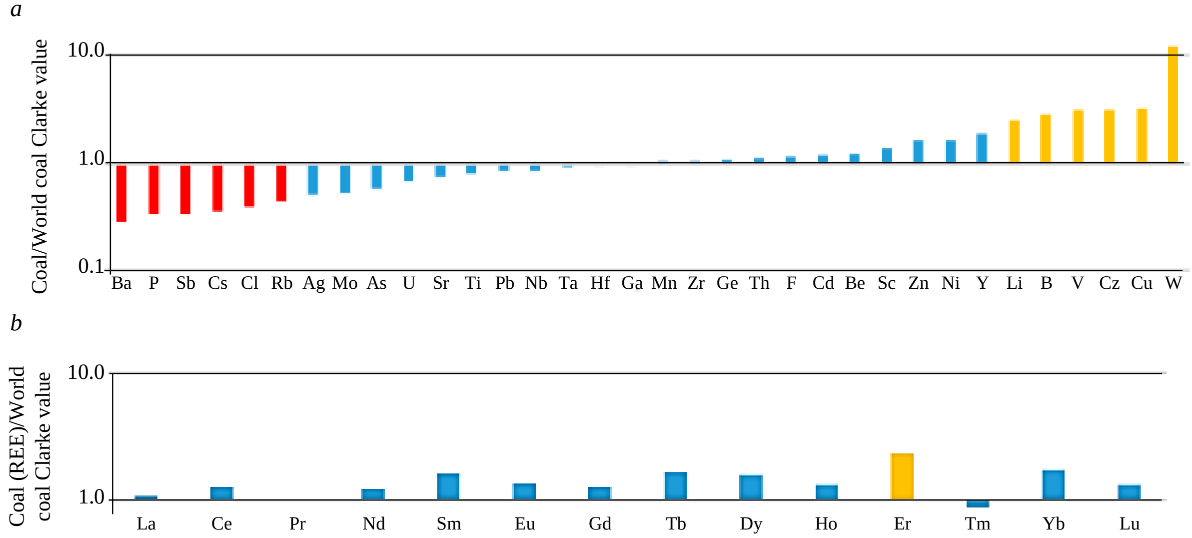

Fig.3. Element concentrations in coals from the Mugun deposit normalized to the world coal Clarke values [13]: *a* – trace elements, arranged in order of enrichment; *b* – rare-earth elements. Element groups are colour-coded according to their Cc: red – depleted (Cc < 0.5), blue – comparable (0.5 ≤ Cc ≤ 2), and yellow – enriched to the world coal Clarke values (Cc > 2)

containing up to 7 % F and approximately 2 % Sr (Fig.4, *h*), sphalerite containing Fe (Fig.4, *i*), galena with chalcopyrite inclusions (Fig.4, *k*), and aggregates of barite containing Sr and Ca together with pyrite (Fig.4, *j*).

Previous SEM studies [8] identified relatively large kaolinite particles, quartz grains, isolated grains of zircon, barite, and sphalerite, pyrite framboids, ilmenite with the composition $(Fe_{0.98}(Mg, Co)_{0.04})_{1.02}TiO_3$ [14], and monazite [7] in coals from the Mugun deposit. Plagioclase, micas, and hematite were identified in the coal ashes [8].

Principal component analysis. PCA was performed to identify the main factors controlling the distribution of trace elements in the coals and host rocks. This statistical method reduces the dimensionality of multivariate data and reveals the principal trends in their variation. The analysis was carried out in two stages. The first stage included both coals and terrigenous interlayers, represented by 74 and 15 samples, respectively (Fig.5, *a*, *b*). The second stage included only coal samples analyzed for an extended suite of elements, including REE, and comprised 11 samples (Fig.5, *c*). On the loading plot for the first and second principal components, which account for 55.62 and 9.03 % of the total variance, respectively, elements positively loaded on the first principal component are separated and correlate with total ash yield A. The vector of total ash yield and the associated elements is directed toward the field of terrigenous rock interlayers (Fig.5, *b*), because their concentrations increase in these samples. The strongest correlations with total ash yield, at $p < 0.0001$, are observed for Ti 0.95; Cl 0.95; Rb 0.94; Cr 0.93; Nb 0.91; Ga 0.90; Ag 0.90; Cs 0.90; Zr 0.90; Hf 0.89; Li 0.87; Ba 0.85; Ta 0.85; Pb 0.82 and F 0.88. This suggests, on the one hand, a clastic origin for these elements and, on the other, a probable commonality of the epigenetic transformations affecting the coals and terrigenous rock interlayers.

Be, P, Sc, V, Fe, Ni, Zn, Y, Sn, Th, and U have correlation coefficients greater than 0.56 with total ash yield at $p < 0.0001$. B has a pronounced negative loading on the first principal component, whereas Sr and S show weak negative or positive loadings. The vectors of these elements, by contrast, are directed toward the field of low-ash coals and are probably associated with the organic fraction. Cu and Cd have high positive loadings on the second principal component, whereas S and B show pronounced negative loadings. The loadings on the second principal component of elements strongly correlated with total ash yield are close to zero. Notably, B has a clear negative loading on both principal components considered.

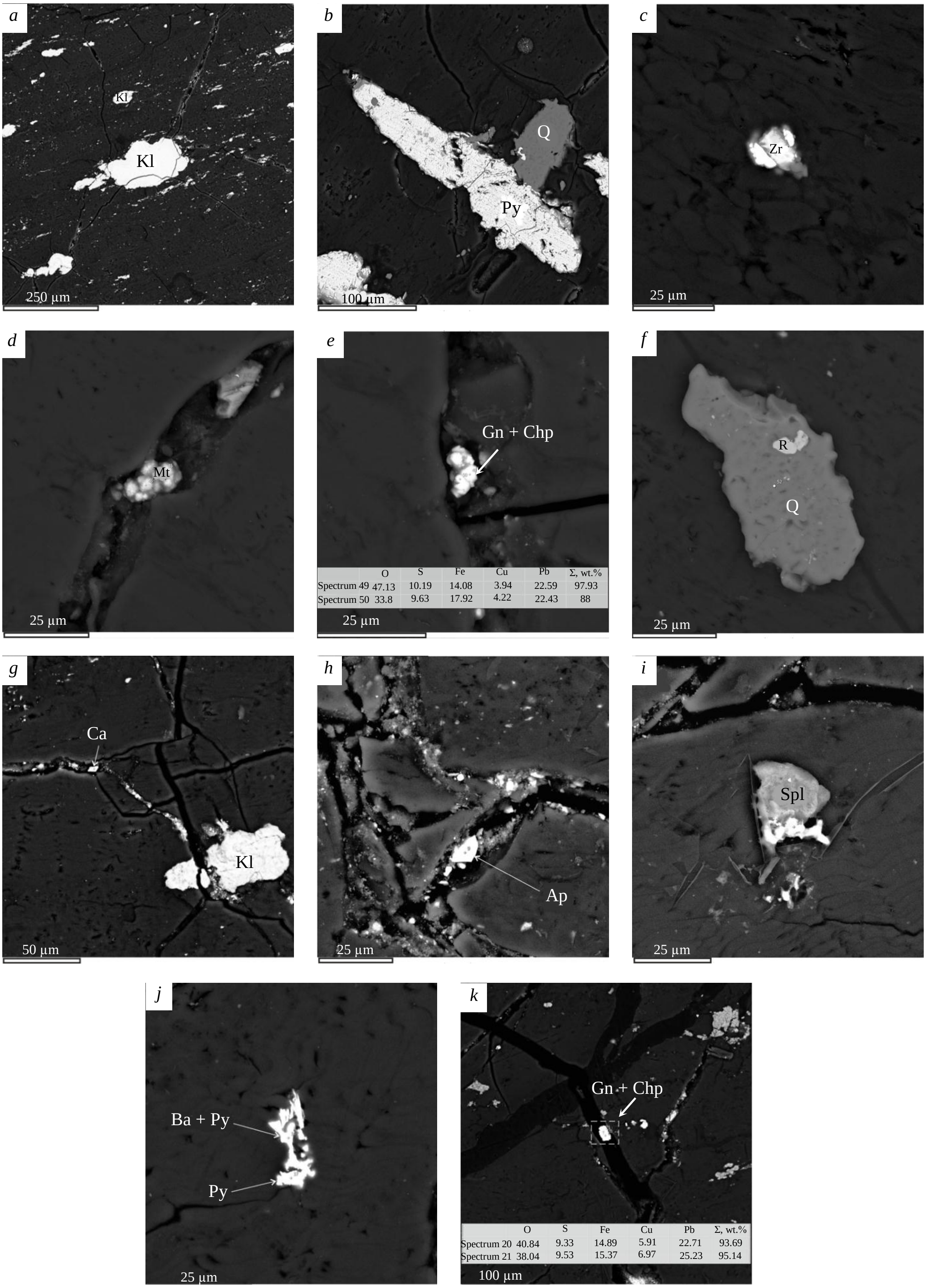

Fig.4. Allogenic and authigenic minerals in coals from the Mugun deposit: *a* – kaolinite; *b* – quartz and pyrite; *c* – zircon; *d* – magnetite; *e* – oxidized galena (anglesite?) containing chalcopyrite inclusions; *f* – quartz containing a rutile inclusion; *g* – calcite and kaolinite; *h* – apatite; *i* – sphalerite; *j* – barite-pyrite aggregate; *k* – galena containing chalcopyrite inclusions. Samples: *a*, *g*-*k* – Mu-D-B5-2-2 (Seam I); *b* – Mu-D-B2-2-2 (Seam II); *c*-*f* – Mu-D-B3-2-1 (Seam II)

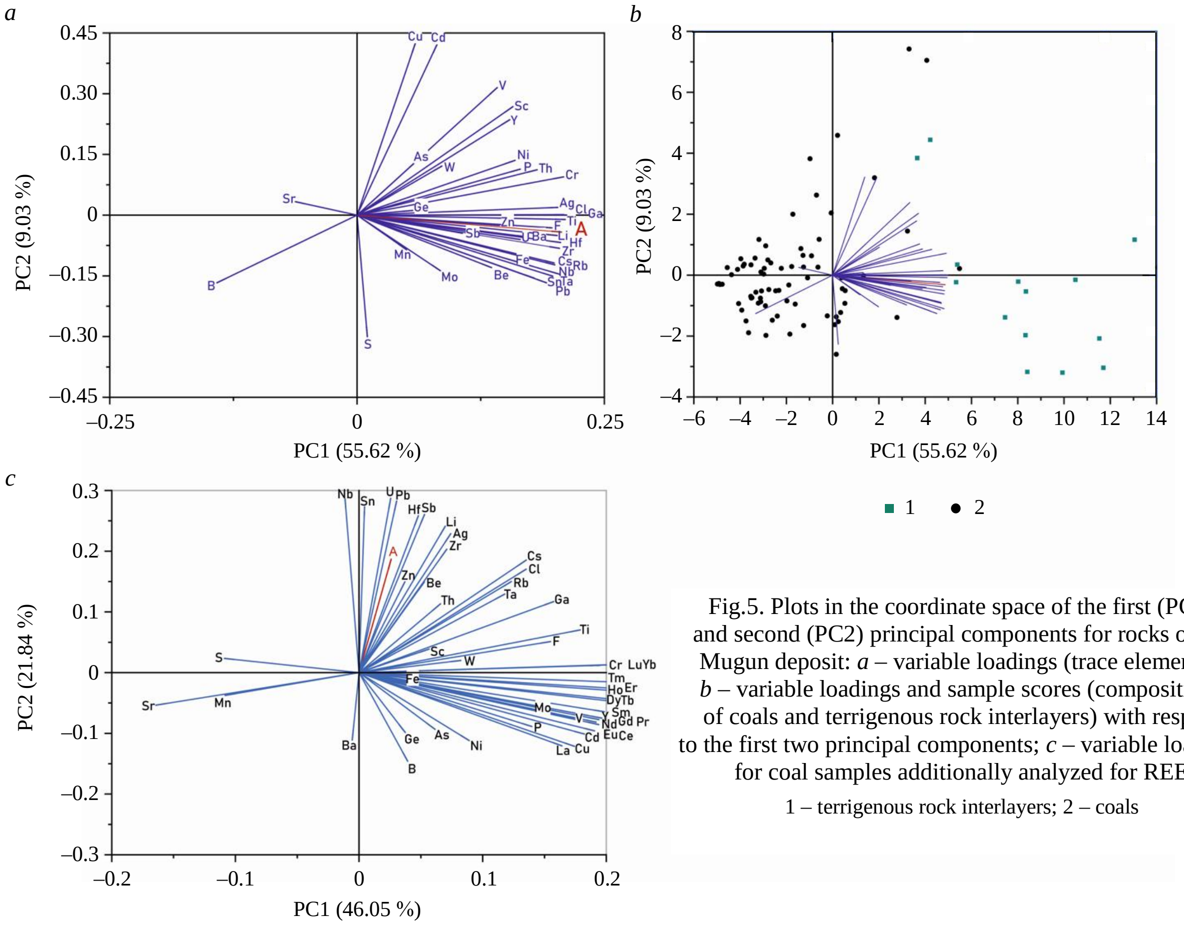

Fig.5. Plots in the coordinate space of the first (PC1) and second (PC2) principal components for rocks of the Mugun deposit: *a* – variable loadings (trace elements); *b* – variable loadings and sample scores (compositions of coals and terrigenous rock interlayers) with respect to the first two principal components; *c* – variable loadings for coal samples additionally analyzed for REE

1 – terrigenous rock interlayers; 2 – coals

The PCA plot constructed for coal samples only, with the REE dataset included, is shown in Fig.5, *c*. Elements strongly correlated with total ash yield have low loadings on the first principal component, which accounts for 46.05 % of the total variance. The highest loadings are shown by the REE, as well as by P, Cu, Cd, Mo, V, Cr, Cs, Cl, Rb, Ta, Ga, Ti, and F. Sr, Mn, and S have distinct negative loadings on the first principal component. On the second principal component, which explains 21.84 % of the variance, the highest positive loadings are shown by Li, Be, Zn, Zr, Nb, Ag, Sn, Sb, Hf, Pb, and U. Negative loadings are observed for B, P, Ni, Cu, Ge, As, Cd, Ba, and the light REE.

Discussion

Modes of occurrence of chemical elements. When coals and terrigenous rock interlayers are analyzed jointly (Fig.5, *a*, *b*), the first principal component clearly separates elements associated with total ash yield and tending toward the host-rock compositions from B on the opposite side. Along the second principal component, B likewise has a strong negative loading, unlike the other variables considered, together with S, which shows a weak positive loading on the first component. Cu and Cd display high positive loadings on the second principal component.

Coal-affinitive elements form stable chemical compounds with organic matter. In general, trace-element enrichment in coal may be represented by the following theoretical models: enrichment by terrigenous clastic material, enrichment by pyroclastic material, enrichment associated with infiltration and groundwater, and fluid-related enrichment (exudation enrichment) caused by the upward migration of fluids of various origins [15]. For elements associated with total ash yield, the composition of the ash should be considered in greater detail. The principal carriers of coal-affinitive elements in coal are sorption ash (Be, Ge, Ba, Sr, Mo), clastogenic ash (Mn, Ga, V, Cr, Ti, Zr), and biogenic ash, in which B predominates and Cu, Mn, Zn, Co, and Mo may also occur; diagenetic and epigenetic ashes are characterized by variable impurity contents [16]. Empirical models of rare-element distribution in ash reported in the literature [16] suggest that the group of elements with positive loadings on the first principal component is dominated by clastogenic carriers, with some contribution from diluting ash. Such diluting ash may also contain these elements, but in substantially lower amounts. Apparently, clastogenic, diagenetic, and epigenetic ash components, including authigenic minerals developed in rock fractures, all contribute to total ash yield. Sulfur occurs both in the carbonaceous matter itself and in authigenic minerals and therefore has a loading close to zero. The interpretation of the positive loading on the second principal component is less straightforward, particularly because this component accounts for less than 10 % of the total variance.

The PCA results for coal samples alone (Fig.5, *c*) should now be considered. The correlation with P and the pronounced positive loading on the first principal component indicate that phosphates are the principal carriers of light REE. Apatite was identified both in the present study and in earlier work, and monazite has also been reported. Laboratory model experiments have shown that peat, lignite, and their organomineral constituents have a high capacity to remove all lanthanides from aqueous solutions, while REE sorption by organic-matter components proceeds through physical sorption, ion-exchange reactions involving carboxyl and hydroxyl groups, and complex formation [17]. It may therefore be assumed that some of the REE in the coals of the Mugun deposit are associated with organic matter.

Other elements with pronounced positive loadings on the first principal component and their probable carriers include: Cs – clay minerals, feldspars, and micas; Cl – apatite and compounds associated with organic matter; Rb – clay minerals and micas; Ta – oxides; Ga – clay minerals, compounds associated with organic matter, and sulfides; Ti – oxides (particularly rutile), clay minerals, and compounds associated with organic matter; F – apatite, clay minerals, micas, and compounds associated with organic matter; Cr – clay minerals, magnetite, and rutile; V – clay minerals, magnetite, rutile, and sulfides; and Mo – sulfides and compounds associated with organic matter. Thus, the strong positive loading on the first principal component appears to reflect several factors operating simultaneously: phosphates, clay minerals, in this case primarily kaolinite, and, to some extent, compounds associated with organic matter. The latter interpretation is indirectly supported by the low but positive loading of B on the first principal component. Some trace elements, for example Cu, are probably supplied to the coals of the Mugun deposit predominantly through carbonaceous matter [18].

Negative loadings on the first principal component are observed for S, Sr, and Mn. Sulfur shows relatively high correlation coefficients with Sr 0.65, and Mn 0.50. This may indicate that the negative loading reflects the occurrence of these elements in sulfates; Ba also has a weak negative loading. Alternatively, Sr and Mn may occur in organic matter as biophile elements. The influx of sulfates from waters circulating through anhydrite-bearing underlying rocks of the Moty Formation into the peat-forming environment was previously discussed for the deposits under study [7]. According to those data, sulfide sulfur predominates in coals from the Mugun deposit and occurs mainly in pyrite and marcasite, with rarer sphalerite, galena, and chalcopyrite inclusions. Sulfates are represented by anhydrite and, less commonly, barite, whereas organic sulfur averages 0.84 %. According to our SEM data, sulfur concentrations in carbonaceous matter range from 1.74 to 5.3 % in sample Mu-D-B5-2-2 from Seam I and reach 0.93 % in sample Mu-D-B3-2-1 from Seam II (Fig.6). This suggests that organic sulfur may play a substantial role in individual samples from Seams I and II. However, local sulfur concentrations of up to 5.3 % in carbonaceous matter obtained by SEM-EDX require cautious interpretation. They probably reflect not only organically bound sulfur, but also the presence of submicron sulfide inclusions that cannot be resolved by SEM.

The highest loadings on the second principal component, exceeding even that of total ash yield, are shown by typical clastophile elements, which may occur, for example, in zircon, including Nb, Sn, Hf, Be, U, and Zr, as well as by elements characteristic of sulfides such as sphalerite and galena. Sulfur has a weak positive loading because it occurs both in the carbonaceous matter itself and in sulfates. Pronounced negative loadings on the second principal component are shown by B, P, Ni, Cu, Ge, As, Cd, Ba, and some light REE. For these elements, several carrier phases may therefore be inferred, with a dominant contribution from their occurrence in carbonaceous matter.

Journal of Mining Institute. 2026. Vol. 280. P. 85-103

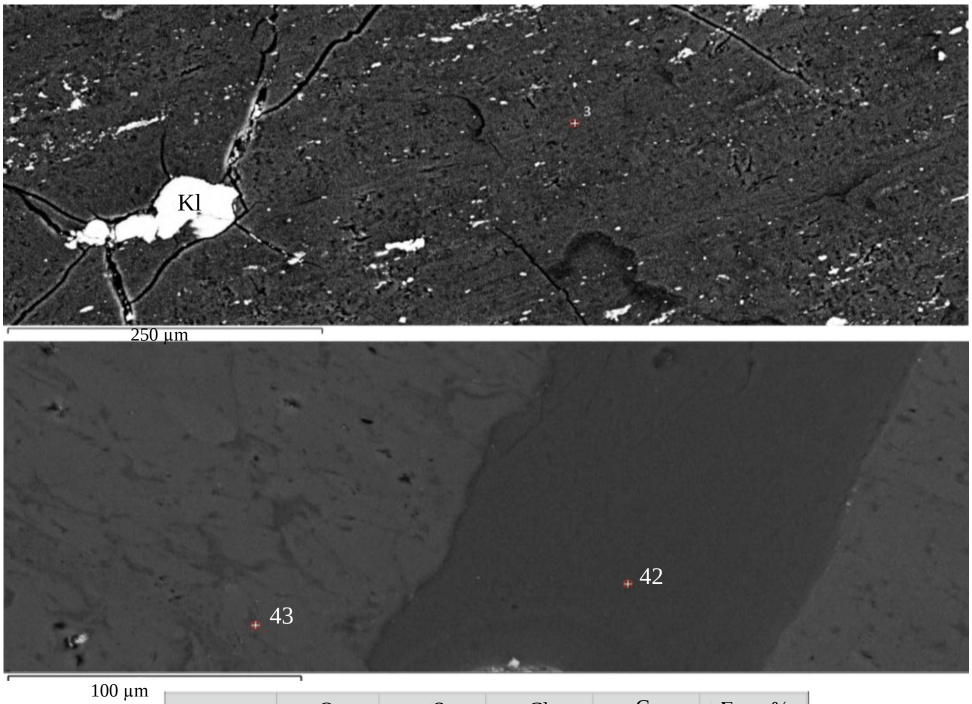

	O	S	Cl	Ca	Σ, wt.%
Spectrum 3	6.73	5.3		0.88	12.91
Spectrum 42	1.92		0.25		2.17
Spectrum 43	5.09	0.93		0.77	6.79

Fig.6. Coal-affinitive trace elements in carbonaceous matter.
Images were acquired using an LE-BSE detector

Sediment provenance inferred from geochemical data. A synthesis of published data makes it possible to identify the principal factors controlling the input and accumulation of trace elements in coal-bearing sequences [19].

Composition of the source-rock assemblage. The geochemical specialization of coal largely reflects the composition of bedrock in the source area. Where felsic igneous and metamorphic complexes predominate, elements characteristic of these rocks become more important, whereas carbonate- or mafic-dominated source areas produce different elemental associations. Geochemical zonation may occur within a single basin as a result of spatial and temporal changes in sediment sources [20, 21].

Weathering crusts. The maturity of terrigenous material and the intensity of weathering of source rocks determine the chemical composition of detritus entering the peat-forming environment. Mature quartz-kaolinite material is generally depleted in many trace elements, whereas weathering crusts developed on rocks with anomalous geochemical backgrounds may act as independent sources of elevated concentrations of particular elements [16, 22, 23].

Volcanic ash input. Explosive volcanism and episodes of ash fall into peat-forming environments represent an important source of tuff-affinitive elements such as Zr, Hf, REE, Nb, Ta, etc. Repeated ash input may lead to the formation of metal-bearing coals enriched in rare and high-field-strength lithophile elements, while the composition of tonsteins can be used to identify the type of volcanic source [24].

Mineralized waters. Groundwater and surface water draining mineralized areas may transport dissolved components, particularly U, W, and other elements, and generate local anomalies within peatlands. The influence of water-borne input is most pronounced in discharge zones and topographic depressions [19].

Paleogeographic distance and facies conditions of peat accumulation. The distance from the source area, hydrological regime, and type of peatland control both the total terrigenous influx and the degree of geochemical differentiation. In marginal parts of a basin, the contribution of terrigenous material and the concentrations of several elements generally increase, whereas farther from the source area the material becomes more mature and chemically depleted. Such facies-related changes may be expressed both laterally and vertically through the succession [19].

Overall, studies of coals from different regions confirm the key role of terrigenous, including volcanogenic, material in enriching coal seams in rare and dispersed elements [11, 25-27]. The nature of the resulting elemental associations and their concentration levels are controlled by the source type, including the composition of the source-rock assemblage and volcanic ash input [28-30], the intensity of weathering, the magnitude of terrigenous influx, and, in some cases, the influence of external solutions [31, 32].

Russian studies likewise demonstrate the importance of source-area composition. At the Azey deposit of the Irkutsk Coal Basin, anomalous concentrations of several trace elements in coal seams are interpreted mainly in terms of the composition of rocks in the source area. According to published studies [33, 34], possible sources of clastic material for the Azey coals included Riphean and Karelian granitoids of the Proterozoic basement and the weathering crusts developed upon them. These ancient weathered rocks are thought to have supplied REE, Y, U, Th, Ta, and Sn to the coals of the area. Triassic traps, including gabbro-dolerites and dolerites, together with their weathering crusts, also played an important role. These rocks are widespread both on the Angara-Lena Plateau and near the Azey deposit. According to previous authors, these basaltic rocks may have been the principal source of Sc in the Azey coals. Altered volcanogenic pyroclastic interlayers, or tonsteins, have also been identified in the Azey succession [35]. Isotopic and geochemical data indicate that their original material consisted of felsic tuffs [36], which were subsequently altered in the aggressive environment of a peat swamp [37]. This example confirms that, even within a single region, the composition of terrigenous material may vary substantially, from granitic to basaltic rocks and volcanic ash, thereby controlling the geochemical specialization of the coals.

These global patterns make it possible to identify key indicators for diagnosing sediment provenance. For the Mugun deposit, particular attention was therefore paid to elemental ratios indicative of specific source-rock assemblages. To determine the probable sources of sediment during formation of the coal-bearing sequence of the Mugun deposit in the Irkutsk Basin, the geochemical characteristics of terrigenous rock interlayers, represented by siltstones and mudstones occurring between the coal seams, were examined. Because REE in the Mugun coals are concentrated mainly in phosphate minerals, particularly apatite, REE patterns and anomalies are difficult to use for provenance analysis. Instead, relatively immobile lithophile high-field-strength elements associated with clastic material were selected, including Zr, Ti, Nb, Sc, Th, and Y. Their concentrations and ratios in the clastogenic interlayers make it possible to reconstruct the composition and type of source rocks.

On the Zr/Sc – Th/Sc diagram (Fig.7, *a*), the data points representing the terrigenous interlayers of the Mugun succession plot outside the field of repeated sedimentary recycling. In other words, the Th/Sc and Zr/Sc ratios do not indicate a substantial contribution from reworked sedimentary rocks. Instead, the values are consistent with first-cycle sedimentation, in which clastic material was supplied directly from primary bedrock without a prolonged prior history of sedimentary reworking. The geochemical data may therefore be interpreted as reflecting direct erosion and transport of igneous and metamorphic rocks into the depositional basin rather than recycling of pre-existing sedimentary sequences.

On the Nb/Y – Zr/TiO_2 diagram (Fig.7, *b*), which is commonly used to evaluate the petrogenetic character of source rocks, most samples from the rock interlayers plot within the field of intermediate-composition rocks, namely andesites and diorites. This suggests that the principal source rocks were probably volcanic or plutonic rocks of andesitic composition. Some samples, however, are shifted toward the field of felsic rocks, including rhyodacites, dacites, and granodiorites. These include the siltstone from the roof of Seam I, sample M-D-2-1-1, and the carbonaceous siltstone from the floor of Seam I in the central part of the deposit, sample M-D-B16-1-4. This indicates an episodic contribution

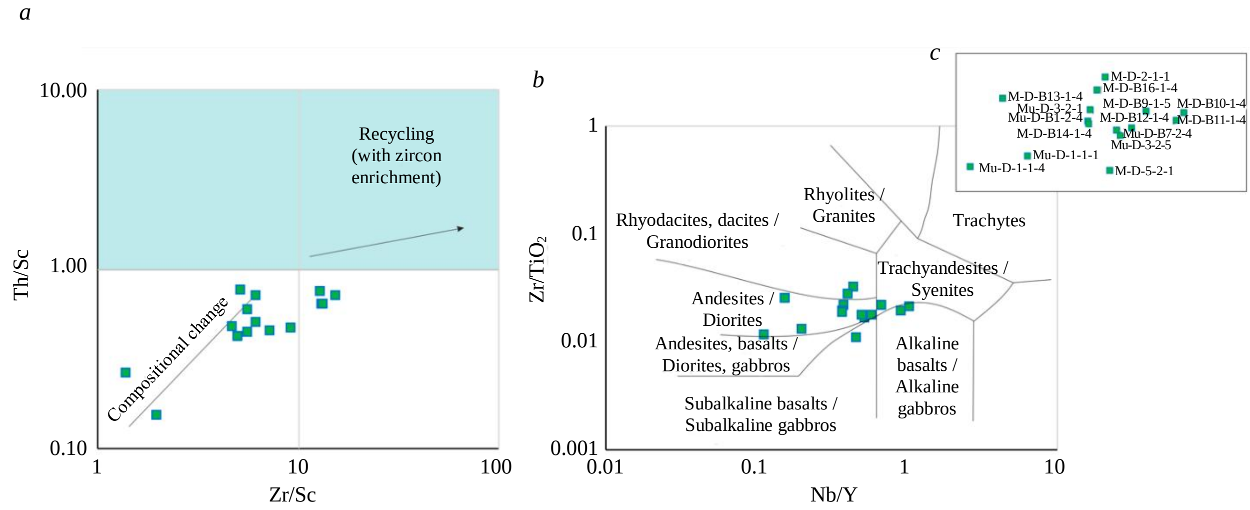

Fig.7. Compositions of the host rocks from the Mugun deposit plotted on: *a* – the Zr/Sc – Th/Sc diagram [15]; *b* – the Nb/Y – Zr/TiO_2 diagram [38]; *c* – inset showing the data-point numbers in Fig. *b*

of more felsic material. Several other samples display elevated Nb/Y ratios and lower Zr/TiO_2 values and plot in the fields of alkaline and subalkaline basalts and their gabbroic equivalents. These include the siltstone from the roof of Seam II, sample M-D-5-2-1, and the siltstones from the floor of Seam I, samples M-D-B10-1-4 and M-D-B11-1-4. Some of these points also tend toward the trachydacite – trachyandesite and syenite fields (for example, M-D-B10-1-4, M-D-B11-1-4, and M-D-B9-1-5 lie near the boundary between the basaltic and trachytic fields). Thus, the geochemical diagram indicates a mixed provenance: rocks of intermediate, mainly andesitic, composition were dominant, but felsic material and basaltic rocks, including alkaline varieties, also contributed.

It should be noted that the siltstone samples designated as the “roof” and “floor” of coal seams, including M-D-2-1-1 and M-D-5-2-1, etc. represent independent lithological units of the host-rock sequence adjacent to the coal benches and are not part of the coal seams in the strict stratigraphic sense. Accordingly, these samples are hereafter treated as host siltstones reflecting depositional conditions distinct from those under which the coals themselves formed.

The potential source-rock types identified from the geochemical data are in good agreement with the geological structure of the areas surrounding the Mugun deposit. Igneous complexes ranging in age from the Paleozoic to the Mesozoic are widely developed in the foothills of the Eastern Sayan in southern Cisbaikalia, which surround the basin. Late Paleozoic-Triassic volcano-plutonic belts occur in southwestern Irkutsk Region and adjacent areas and include orogenic andesites and diorites. More evolved felsic plutons are also known in the region, including granitoids, rhyodacites, dacites, and granodiorites, commonly associated with local domal structures such as the Sayan granitoid massif. These rocks correspond to the felsic component of the source province. In addition, lava flows and intrusions of the Late Permian-Triassic trap complex are present in the adjacent region and consist of subalkaline basalts and gabbrodolerites. They are associated with rift structures and plateaus, including the Angara-Lena Plateau, and correspond to the basaltic component inferred from the geochemical data. Rare occurrences of Late Paleozoic – Mesozoic trachyte-trachyandesite-syenite intrusive complexes, including nepheline syenites and other alkaline varieties, are also known within various blocks of the Eastern Sayan foothills. Their presence is consistent with the trachytic, alkaline component identified in the clastic material of the Mugun deposit. Thus, the full range of rock types indicated by the Nb/Y – Zr/TiO_2 diagram has geological counterparts among the regional igneous complexes, supporting the reliability of the geochemical provenance reconstruction.

Conclusions

The complex multidimensional system describing the carrier phases of rare elements in coal is difficult to represent adequately by deliberately projecting a data cloud into a low-dimensional space with only two coordinate axes. Consequently, several factors may contribute simultaneously to a given principal component. Ash yield itself is the sum of heterogeneous components. Elements associated with the organic fraction of coal are concentrated most strongly in the ash, whereas elements occurring exclusively in the inorganic fraction are not enriched in ash relative to the host rocks and may even be depleted [17]. As established previously [6], the ash and slag produced from Mugun coal are enriched relative to the coal most strongly in Cu (up to 40 times), Fe (6-40 times), Ba (12-48 times), as well as Nb (3-8 times), Sr (4-12 times), As (up to 4 times), Pb (2-16 times), Zn (4-21 times), Cr (3-9 times), V (up to 6 times), Ti (4-10 times), U (up to 9 times), and Th (up to 13 times).

Based on the evidence considered above, the following assumptions may be proposed:

• Li, Be, Zn, Zr, Nb, Ag, Sn, Sb, Hf, Pb, and U occur in the clastic fraction and in sulfides;

• F, Cl, Ti, Ga, Rb, Cs, Ta, and Th are associated with clay minerals, compounds bound to organic matter, and sulfides;

• P, V, Cr, Cu, Mo, Cd, and REE are associated with phosphates and compounds bound to organic matter;

• B, S, Mn, Ni, Ge, As, Sr, and Ba are associated with sulfates and compounds bound to organic matter, with a possible minor contribution from sulfides.

On the Nb/Y – Zr/TiO_2 diagram (Fig.7, *b*), the silty varieties of the host-rock sequence adjacent to the coal seams of the Mugun deposit display a broader compositional range than the coals. Some samples plot within the field of intermediate-composition rocks, namely andesites and diorites, whereas others tend toward felsic rhyodacite-dacite compositions or, conversely, toward more alkaline, including subalkaline, basaltic varieties. This suggests differentiation of the sources of clastic material between different parts or stratigraphic levels of the succession:

• Samples M-D-2-1-1 (a host-rock siltstone adjacent to the roof of Seam I), and M-D-B16-1-4 (a carbonaceous siltstone from the floor of Seam I) plot in the rhyodacite-dacite field, close to granitoid compositions. The probable sediment source was erosion of granitoid, including granodioritic and dacitic, massifs in the foothills of the Eastern Sayan, formed during Paleozoic-Mesozoic orogenic stages. Given the location of the deposit, the most likely influence was from granitoids of the Sayan complex, exposures of which are known in the central and southwestern parts of the region.

• Samples M-D-5-2-1 (a host-rock siltstone adjacent to the roof of Seam II) and M-D-B10-1-4 and M-D-B11-1-4 (siltstones from the floor of Seam I) plot within the alkaline and subalkaline basalt/gabbro fields (samples M-D-B10-1-4 and M-D-B11-1-4 show a transition toward trachyandesites and syenites). These geochemical characteristics may indicate a contribution from rocks related to subalkaline basaltic and syenitic magmatism. In the region, such igneous formations are associated particularly with Late Paleozoic and Mesozoic magmatic phases and with local alkaline massifs, including the Ziminsky and Ognitsky complexes. Such material could have been supplied through erosion of gabbroic intrusions and/or volcanic flows developed along the periphery of the Eastern Sayan.

• Sample M-D-B9-1-5 is similarly displaced toward the trachyandesite and syenite fields, likewise indicating an alkaline or subalkaline character of the source province.

Thus, the host rocks of the productive seams at the Mugun deposit contain multicomponent clastic material and collectively indicate a polygenetic source of the sandy-silty detritus. This material was supplied from the west and southwest from granitoid domes and batholiths of the Sayan orogenic belt, represented by the granodiorite-dacite association, and from the east and northeast from local alkaline and subalkaline massifs in the foothills of the Eastern Sayan, including the Ziminsky and Ognitsky complexes. The following principal conclusions can therefore be drawn:

• The mineralogical and geochemical characteristics of the Mugun coals are controlled by a combination of allogenic and authigenic phases, including kaolinite, zircon, rutile, pyrite, sphalerite, apatite, barite, and other minerals identified by scanning electron microscopy and energy-dispersive X-ray analysis.

• Trace elements in the coals occur in several types of carriers: clastogenic, phosphate, sulfide, and organic. The most important carrier phases include clay minerals (especially kaolinite), phosphates (apatite and monazite), sulfides (pyrite, galena, and sphalerite), and organic matter.

• Principal component analysis identified statistically significant groups of elements correlated with total ash yield, making it possible to distinguish elements according to their origin and accumulation conditions: clastogenic elements are associated mainly with terrigenous rocks, whereas organophilic elements tend toward low-ash coals.

• Discriminant geochemical analysis using the Nb/Y – Zr/TiO_2 and Zr/Sc – Th/Sc diagrams showed that the sources of sediment supplied to the coal-bearing succession of the Cheremkhovskaya Formation were polygenetic and included granitoids, felsic volcanic rocks, and subalkaline volcanic rocks from the foothills of the Eastern Sayan.

The authors thank the staff of EN+ COAL LLC for their assistance in collecting the study material and for supporting the research. The authors also express their sincere gratitude to Ya.E.Yudovich for his valuable advice and consultations.

REFERENCES

1. Krasnov O.S., Salikhov V.A. Prospects of producing scarce non-ferrous and less-common metals from coal wastes in Kuzbass. *Tsvetnye metally*. 2007. N 8, p. 8-11 (in Russian).

2. Arbuzov S.I., Ershov V.V., Potzeluyev A.A., Rikhvanov L.P. Rare elements in Kuznetsk basin coals. Kemerovo: Kemerovskii poligrafkombinat, 2000, p. 248 (in Russian).

3. Krasnov O.S., Salikhov V.A. Economical valuation of coal fields useful coproducts. *Journal of Mining Institute*. 2013. Vol. 201, p. 196-200 (in Russian).

4. Jaiswal H., Singh A.K. Coal as a non-conventional resource of rare earth elements (REEs) and trace elements: Benefits and impacts on environment and human health – A review. *Results in Earth Sciences*. 2025. Vol. 3. N 100064. DOI: 10.1016/j.rines.2025.100064

5. Pogrebitskii E.O. Some regularities of germanium distribution in coals of the Donets Basin. *Journal of Mining Institute*. 1959. Vol. 35. Iss. 2, p. 87-103 (in Russian).

6. Bembeev D.B., Samsonov A.A. Geochemical characterization of ash and slag from coals of the Mugun deposit (Irkutsk region). *Nedropolzovanie XXI vek*. 2024. N 2 (103), p. 28-35 (in Russian).

7. Dzhumayan N.R. Formation conditions and qualitative composition of lignite from the Mugun deposit (Irkutsk coal basin): Avtoref. dis. … kand. geol.-mineral. nauk. Rostov-na-Donu: Yuzhnyi federalnyi universitet, 2022, p. 26.

8. Dzhumayan N.R., Shumilova T.G., Svetov S.A. Impurity Elements in Coals from the Mugunsk Deposit (Irkutsk Coal Basin). *Solid Fuel Chem*. 2021. Vol. 55. N 6, p. 407-413. DOI: 10.3103/S0361521921060045

9. Coal Resources of Russia. In 6 volumes. Vol. III. Coal Basins and Deposits of Eastern Siberia. Southern Part (Krasnoyarsk Territory, Kansk-Achinsk Basin; Republic of Khakassia, Minusinsk Basin; Republic of Tuva, Ulug-Khem Basin and other deposits; Irkutsk Region, Irkutsk Basin and coal deposits of the Cis-Baikal region) / Editor-in-Chief V.F.Cherepovskii. Moscow: Geoinformtsentr, 2002, p. 488.

10. Gosudarstvennaya geologicheskaya karta Rossiiskoi Federatsii. Masshtab 1:1,000,000 (trete pokolenie). Seriya Angaro-Eniseiskaya. List N-47 – Nizhneudinsk. Obyasnitelnaya zapiska. St. Petersburg: Kartograficheskaya fabrika VSEGEI, 2012, p. 652.

11. Ziyi Ye, Baoqing Li, Jialiang Cao. Enrichment characteristics and genesis mechanism of critical elements (Nb-Ta-Zr-Hf-REE-Y) in coals: a case study of Late Permian coalfield in Northeastern Guizhou, China. *Frontiers in Earth Science*. 2024. Vol. 12. N 1520502. DOI: 10.3389/feart.2024.1520502

12. Timofeev P.P. Jurassic coal measures in Southern Siberia and conditions of its formation. Moscow: Nauka, 1970, p. 207 (in Russian).

13. Yudovich Ya.E., Ketris M.P. Valuable Trace Elements in Coal. Ekaterinburg: Ural Division of the Russian Academy of Sciences, 2006, p. 538 (in Russian).

14. Dzhumayan N.R., Nastavkin A.V. Scanning Electron Microscopy of Pyrite from Brown Coal (Mugun Coal Deposit, Irkutsk Basin). Minerals: Structure, Properties, Methods of Investigation. Springer, 2020, p. 29-34. DOI: 10.1007/978-3-030-00925-0_5

15. McLennan S.M., Taylor S.R., McCulloch M.T., Maynard J.B. Geochemical and Nd–Sr isotopic composition of deep-sea turbidites: Crustal evolution and plate tectonic associations. *Geochimica et Cosmochimica Acta*. 1990. Vol. 54. Iss. 7, p. 2015-2050. DOI: 10.1016/0016-7037(90)90269-Q

16. Yudovich Ya.E. Geochemistry of fossil coals. Leningrad: Nauka, 1978, p. 262.

17. Pavlova L.M., Shumilova L.P., Radomskaya V.I. et al. Sorption of Rare Earth Elements by Organic Matter from Aqueous Solutions according to Experimental Data. *Doklady Earth Sciences*. 2023. Vol. 512. Iss. 2, p. 946-952. DOI: 10.1134/S1028334X23601207

18. Dzhumayan N.R., Silaev V.I., Vasiliev E.A. et al. Mineralogical and geochemical properties of coals of the Mugun deposit (Irkutsk coal basin). *Vestnik of Geosciences*. 2022. N 2 (326), p. 19-36 (in Russian). DOI: 10.19110/geov.2022.2.3

19. Yudovich Ya.E., Ketris M.P. Inorganic matter of coal. Ekaterinburg: Ural Division of the Russian Academy of Sciences, 2002, p. 424 (in Russian).

20. Foscolos A.E., Goodarzi F., Koukouzas C.N., Hatziyannis G. Reconnaissance study of mineral matter and trace elements in Greek lignites. *Chemical Geology*. 1989. Vol. 76. Iss. 1-2, p. 107-130. DOI: 10.1016/0009-2541(89)90131-9

21. van der Flier-Keller E., Goodarzi F. Geological controls on major and trace element characteristics. Cretaceous coals of Vancouver Island, Canada. *Bulletin de la Société Géologique de France*. 1991. Vol. 162. N 2, p. 255-265.

22. Arbuzov S.I., Levitskii V.M. Radiogeochemical correlation of granites of Sayansky and Taraksky complex at the south-west boundary of the Siberian platform. Radioaktivnost i radioaktivnye elementy v srede obitaniya cheloveka: Materialy mezhdunarodnoi konferentsii, posvyashchennoi stoletiyu so dnya otkrytiya yavleniya radioaktivnosti i stoletiyu Tomskogo politekhnicheskogo universiteta, 22-24 maya 1996, Tomsk, Rossiya. Tomsk: Natsionalnyi issledovatelskii Tomskii politekhnicheskii universitet, 1996, p. 86-89 (in Russian).

23. Likhachev V.V. Rare-metal mineralization of the bauxite-bearing weathering crust of the Middle Timan. Syktyvkar: Komi nauchnyi tsentr UrO RAN, 1993, p. 224.

24. Seredin V.V., Finkelman R.B. Metalliferous coals: A review of the main genetic and geochemical types. *International Journal of Coal Geology*. 2008. Vol. 76. Iss. 4, p. 253-289. DOI: 10.1016/j.coal.2008.07.016

25. Biswas S., Moroeng O.M., Wagner N.J. Mineralogy and geochemical controls on the distribution of REY-Ga-Se-Nb enrichment in the No. 6 Coal Seam, Soutpansberg Coalfield, South Africa. *Ore Geology Reviews*. 2024. Vol. 174. N 106310. DOI: 10.1016/j.oregeorev.2024.106310

26. Zhanming Guo, Beilei Sun, Chao Liu et al. Geochemistry of tonsteins and its implications for Li-Zr (Hf)-Nb (Ta) enrichments in Cisuralian coal seams, Shanxi Province, North China. *International Journal of Coal Geology*. 2025. Vol. 300. N 104697. DOI: 10.1016/j.coal.2025.104697

27. Qiuchan Han, Jingjing Liu, Niande Shang et al. Mineralogy and geochemistry of the Middle Jurassic coal in the southern Ordos Basin, China: Responses of element geochemical behavior to climatic changes. *Palaeogeography, Palaeoclimatology, Palaeoecology*. 2024. Vol. 648. N 112284. DOI: 10.1016/j.palaeo.2024.112284

28. Bo Jiu, Wenhui Huang, Nana Mu. Mineralogy and elemental geochemistry of Permo-Carboniferous Li-enriched coal in the southern Ordos Basin, China: Implications for modes of occurrence, controlling factors and sources of Li in coal. *Ore Geology Reviews*. 2022. Vol. 141. N 104686. DOI: 10.1016/j.oregeorev.2021.104686

29. Yang Lin, Jing Li, Xuanphu Nguyen et al. Enrichment of rubidium and cesium in upper Triassic coals from the Cam Pha coalfield, NE Vietnam: Implications on sediment source and hydrothermal influence. *Ore Geology Reviews*. 2025. Vol. 178. N 106484. DOI: 10.1016/j.oregeorev.2025.106484

30. Jidun Sha, Jian Chen, Bofei Zhang et al. Geochemistry of source rock–controlled Late Triassic coal: An example from the Dabaoding Coal Mine in Panzhihua, Sichuan Province, southwestern China. *International Journal of Coal Geology*. 2020. Vol. 221. N 103431. DOI: 10.1016/j.coal.2020.103431

31. Niande Shang, Jingjing Liu, Qiuchan Han et al. Mineralogy and geochemistry of the Middle Jurassic coal from the Hexi Mine, Shenfu Mining Area, Ordos Basin: With an emphasis on genetic indications of siderite. *International Journal of Coal Geology*. 2023. Vol. 279. N 104384. DOI: 10.1016/j.coal.2023.104384

32. Yang Wang, Manli Huang, Yanming Zhu et al. Mineralogy, geochemistry and enrichment mechanism of critical elements (Li and Zr-Nb-Hf-Ta-REY) in the coals from western Guizhou Province, China: Source and sedimentary environment. *Ore Geology Reviews*. 2025. Vol. 176. N 106402. DOI: 10.1016/j.oregeorev.2024.106402

33. Ilenok S.S., Arbuzov S.I. Metalliferous coals of the Azeyskoe deposit of Irkutsk coal basin. *Bulletin of the Tomsk Polytechnic University. Geo Assets Engineering.* 2018. Vol. 329. N 8, p. 132-144 (in Russian).

34. Ilenok S.S., Arbuzov S.I. Mineral modes of rare elements in coals and ashes of coals of Azey deposit in Irkutsk coal basin. *Bulletin of the Tomsk Polytechnic University. Geo Assets Engineering.* 2016. Vol. 327. N 2, p. 6-20 (in Russian).

35. Admakin L.A., Portnov A.G. Tonsteins of the Irkutsk basin. *Lithology and Mineral Resources.* 1987. N 3, p. 88-98 (in Russian).

36. Arbuzov S.I., Mezhibor A.M., Spears D.A. et al. Nature of tonsteins in the Azeisk deposit of the Irkutsk Coal Basin (Siberia, Russia). *International Journal of Coal Geology*. 2016. Vol. 153, p. 99-111. DOI: 10.1016/j.coal.2015.12.001

37. Arbuzov S.I., Volostnov A.V., Ilenok S.S., Rybalko V.I. Nature of tonsteins from the Azey deposit of the Irkutsk coal basin. *Izvestiya Tomskogo politekhnicheskogo universiteta*. 2012. Vol. 321. N 1, p. 89-97.

38. Winchester J.A., Floyd P.A. Geochemical discrimination of different magma series and their differentiation products using immobile elements. *Chemical Geology*. 1977. Vol. 20, p. 325-343. DOI: 10.1016/0009-2541(77)90057-2

***Authors*: Danzan B. Bembeev,** *Postgraduate Student* (*Lomonosov Moscow State University*, *Moscow*, *Russia*), *bembeev.danzan@yandex.ru*, *https://orcid.org/0009-0001-3275-7329*, **Sofya I. Merenkova,** *Candidate of Geological and Mineralogical Sciences*, *Researcher* (*Shirshov Institute of Oceanology of RAS*, *Moscow*, *Russia*), *Junior Researcher* (*Schmidt Institute of Physics of the Earth of the RAS*, *Moscow*, *Russia*), *https://orcid.org/0000-0003-3204-4393*, **Aleksei A. Samsonov,** *Candidate of Geological and Mineralogical Sciences*, *Senior Researcher* (*Lomonosov Moscow State University*, *Moscow*, *Russia*), *https://orcid.org/0009-0007-4637-0399*, **Ruslan R. Gabdullin,** *Doctor of Geological and Mineralogical Sciences*, *Professor* (*Lomonosov Moscow State University*, *Moscow*, *Russia*), *Leading Researcher* (*Vernadsky Institute of Geochemistry and Analytical Chemistry of the RAS*, *Moscow*, *Russia*), *https://orcid.org/0000-0001-8296-7191*.

The authors declare no conflict of interests.